J Solid State Electrochem (1997) 1: 134–142

ORIGINAL PAPER

Fritz Scholz · Milivoj Lovrić · Zbigniew Stojek

The role of redox mixed phases $\{ox_x(C_n\,red)_{1-x}\}$ in solid state electrochemical reactions and the effect of miscibility gaps in voltammetry

Received: 9 January 1997 / Accepted: 12 March 1997

Abstract A basic analysis is performed to establish the interrelations between the equilibria existing when one solid phase {ox} is transformed into another solid phase $\{C_n red\}$ while both are in close contact with a solution containing both redox forms in the dissolved state. The transformation of the above solid phases by electrochemical reactions can be understood when the intermediate formation of mixed phases between {ox} and $\{C_n red\}$ is taken into account. Such a description allows solid state electrochemical reactions to be modeled for the case of an infinite miscibility of oxidized and reduced solid compounds as well as for the case of systems with miscibility gaps. It is shown that miscibility gaps will lead to a splitting of both the anodic and cathodic voltammetric peaks and also to a distinct separation of the anodic and cathodic reactions on the potential scale in voltammetric experiments. This phenomenon can be called an immiscibility polarization.

Key words Solid phase · Redox · Transformation · Miscibility · Voltammetry

Introduction

Let {ox} and $\{C_n red\}$ be two solid phases which are both electronic and ionic conductors, and let us assume that both phases are in close contact with an electrolyte solution containing C^+ and also in contact with an electron supplier (three-phase system, cf. Fig. 2), i.e. a metal or graphite electrode. The overall electrochemical reaction can then be formulated for the solid compounds as follows:

$$\{ox\} + ne^- + n[C^+] \rightleftarrows \{C_n red\} \tag{1}$$

Both solid compounds {ox} and $\{C_n red\}$ have a certain solubility in the electrolyte solution. Thus, it is possible to describe the entire system by the following square scheme of equilibria:

Solid state

$$\{ox\} + ne^- + n[C^+] \overset{E^0_{ss}}{\rightleftarrows} \{C_n red\}$$

Solution

$$K_{ox} \qquad\qquad K_{red}$$

$$[ox] + ne^- \qquad\qquad \underset{E^0_{sol}}{\rightleftarrows} [red] + n[C^+]$$

Species enclosed by square brackets are present in the electrolyte solution whereas species enclosed by braces are confined to the solid phase.

Scheme 1

In this scheme, an electrochemical equilibrium is assumed to exist in the solid state which is based on the activities of {ox} and $\{C_n red\}$ in a single solid phase, i.e. a mixed phase with respect to the two oxidation states. The activities of the two redox states are proportional to their formal concentrations in the solid phase. Hence, a Nernst equation can be formulated for this electrochemical equilibrium:

$$E_{ss} = E^0_{ss} + \frac{RT}{nF} \ln \frac{a_{\{ox\}} a^n_{[C^+]}}{a_{\{C_n red\}}} \tag{2}$$

provided that the equilibrium is established within the time scale of the experiment. When the solid compound has a high electronic conductivity, the potential which is

F. Scholz (✉)
Institut für Chemie, Humboldt-Universität, Hessische Str. 1-2, D-10115 Berlin, Germany
e-mail: fritz=scholz@chemie.hu-berlin.de

M. Lovrić
Center for Marine Research, "Rudjer Bošković" Institute, POB 1016, 41001 Zagreb, Croatia
e-mail: slovric@olimp.irb.hr

Z. Stojek
Department of Chemistry, University of Warsaw, Pasteura 1-2, 02-093 Warsaw, Poland
e-mail: stojek@chem.uw.edu.pl

applied to the electrode will be equal to E_{ss} and will, via Eq. 2, determine the ratio of the oxidized to the reduced form in the solid state.

Now it is possible to ascribe to both {ox} and {$C_n$red} a solubility in the electrolyte solution which depends on the activities of {ox} and {$C_n$red} in the mixed crystal:

$$K_{ox} = \frac{a_{\{ox\}}}{a_{[ox]}} \tag{3}$$

$$K_{red} = \frac{a_{\{C_n red\}}}{a_{[red]} a^n_{[C^+]}} \tag{4}$$

The solubility of the two redox forms in the solution is the basis for the establishment of an electrochemical equilibrium in the solution:

$$E_{sol} = E^0_{sol} + \frac{RT}{nF} \ln \frac{a_{[ox]}}{a_{[red]}} \tag{5}$$

From the reaction scheme, it is obvious that K_{ox} and K_{red}will relate E^0_{ss} and E^0_{sol} to each other. In the equilibrium, the potentials of the solid phase and the solution phase are equal, and a combination of Eqs. 2–5 yields

$$E^0_{ss} + \frac{RT}{nF} \ln \frac{a_{\{ox\}} a^n_{[C^+]}}{a_{\{C_n red\}}} = E^0_{sol} + \frac{RT}{nF} \ln \frac{a_{\{ox\}} K_{red} a^n_{[C^+]}}{K_{ox} a_{\{C_n red\}}} \tag{6}$$

$$E^0_{sol} = E^0_{ss} + \frac{RT}{nF} \ln \frac{a_{\{ox\}} a^n_{[C^+]}}{a_{\{C_n red\}}} - \frac{RT}{nF} \ln \frac{a_{\{ox\}} a^n_{[C^+]}}{a_{\{C_n red\}}} + \frac{RT}{nF} \ln \frac{K_{ox}}{K_{red}} \tag{7}$$

$$E^0_{sol} = E^0_{ss} + \frac{RT}{nF} \ln \frac{K_{ox}}{K_{red}} \tag{8}$$

Equation 7 is of fundamental importance, as it shows that for $K_{ox} \ll K_{red}$ the standard potential E^0_{sol} will be smaller than E^0_{ss}. For the opposite case ($K_{ox} \gg K_{red}$), it follows that $E^0_{sol} > E^0_{ss}$.

Since [ox] and [red] are per se very small concentrations, in many cases even completely negligible, it suffices to treat the solid-state redox equilibrium. From Eq. 8, it follows that the ratio of redox species in the solid phase changes with the ratio of the redox species in the solution phase according to:

$$\log \frac{a_{\{ox\}} a^n_{[C^+]}}{a_{\{C_n red\}}} = \frac{E^0_{sol} - E^0_{ss}}{F_N} + \log \frac{a_{[ox]}}{a_{[red]}} \tag{9}$$

$(F_N = RT/nF)$

The treatment of the solid-state electrochemical reaction, proceeding as a continuous transformation of {ox} to {$C_n$red} via mixed phases of the composition $\{ox_x(C_n red)_{1-x}\}$ gives a chance to describe this process on the basis of mixed phase thermodynamics, whereas the assumption of complete immiscibility of {ox} and {$C_n$red} does not allow an equilibrium description, especially when the solubility of ox and red in the electrolyte solution is negligible. Additionally, there exist plenty of experimental proofs that solid state reactions proceed as a continuous transformation of one redox form into another (see e.g. the case of most lithium batteries [1]).

Further, the model of redox mixed phases allows the treatment of miscibility gaps. We can show that miscibility gaps provide a simple and plausible understanding of voltammograms of solid compounds as published elsewhere [2–4].

Theory

Under these assumptions, the redox reaction (Eq. 1) is defined by the following relationships [5]

$$c_{ox} + c_{red} = \rho \tag{10}$$

$$c_{ox} = c_{red} \exp(\varphi) \tag{11}$$

$$\varphi = (nF/RT)(E - E_f) \tag{12}$$

where c_{ox} and c_{red} are formal concentrations of the solid compounds {ox} and {$C_n$red} in the surface layer of the mixed crystal, respectively, and where ρ is a common molar density of the solid particle (in mol/cm^3). These formal concentrations are related to the activities of the compounds {ox} and {$C_n$red} as $f_{ox}c_{ox} = \rho a_{\{ox\}}$ and $f_{red}c_{red} = \rho a_{\{C_n red\}}$. As to f_{ox} and f_{red}, these are the activity coefficients of the oxidized and reduced forms in the solid state. As a first approximation, both activity coefficients have been assumed to be 1. These relationships are the consequence of the assumed proportionality between the activities and the molar fractions of the redox components $a_{\{ox\}} = f_{ox} m_{ox}/(m_{ox} + m_{red})$ and $a_{\{C_n red\}} = 1 - a_{\{ox\}}$, where m_{ox} and m_{red} are numbers of moles of {ox} and {$C_m$red}, respectively. The formal concentrations and the density are defined as $c_{ox} = m_{ox}/V, c_{red} = m_{red}/V$ and $\rho = (m_{ox} + m_{red})/V$, where V is a volume of the solid particle which is assumed to be constant. Furthermore, it is assumed that the activities of dissolved ions at the surface of the solid particle are the same as in the bulk of the electrolyte solution: $a_{[C^+],x=0} = a_{[C^+],\infty}$. So the formal potential of the redox reaction (Eq. 1) is defined as $E_f = E^0_{ss} + (RT/F) \ln a_{[C^+],\infty}$. Initially, a crystal of a pure substance {ox} is brought into firm contact with the electrode surface, which is charged to a constant potential E. The crystal surface is both a good electron conductor and easily approachable by the ions C^+ from the solution. So the Nernst equilibrium (Eq. 11) is readily established at the crystal surface. Because of ion diffusion from the surface towards the crystal center and because of electron conductance, this equilibrium expands throughout the solid particle [6]. If this is achieved, the concentrations of the substances {ox} and {$C_n$red} will be, respectively:

$$c_{ox} = \rho \exp(\varphi)[1 + \exp(\varphi)]^{-1} \tag{13}$$

$$c_{\mathrm{red}} = \rho[1 + \exp(\varphi)]^{-1} \quad (14)$$

Obviously, such a scenario is possible only if the solid compounds {ox} and {$C_n$red} can be mixed in any ratio, i.e. if their molar ratios in the mixed crystal can be continuously changed from zero to one and vice versa. If the solubility of one of these solid compounds in another is limited, the activities of both components can be changed only within a restricted range, and the Nernst equilibrium (Eq. 11) will not be satisfied at all potentials. This leads to the immiscibility polarization which is shown in Fig. 1. If {ox} is gradually reduced to {$C_n$red}, the activity of {$C_n$red} may increase up to a certain limiting value $Z_{\mathrm{red/ox}} = (m_{\mathrm{red}})/(m_{\mathrm{red}} + m_{\mathrm{ox}})$ which depends on the maximum solubility of {$C_n$red} in {ox}. The potential of the saturated mixed crystal is

$$E_{\mathrm{C},1} = E_{\mathrm{f}} + 2.3(RT/nF)\log[(1 - Z_{\mathrm{red/ox}})/Z_{\mathrm{red/ox}}] \quad (15)$$

where $Z_{\mathrm{red/ox}}$ is the maximum solubility of {$C_n$red} in {ox}. The second critical potential depends on $Z_{\mathrm{ox/red}} = (m_{\mathrm{ox}})/(m_{\mathrm{ox}} + m_{\mathrm{red}})$, which is the maximum solubility of {ox} in {$C_n$red}:

$$E_{\mathrm{C},2} = E_{\mathrm{f}} + 2.3(RT/nF)\log[Z_{\mathrm{ox/red}}/(1 - Z_{\mathrm{ox/red}})] \quad (16)$$

The ratio $(a_{\{\mathrm{ox}\}})/(a_{\{C_n\mathrm{red}\}})$ in the crystal can be changed continuously if $E > E_{\mathrm{C},1}$ and if $E < E_{\mathrm{C},2}$, but from $E_{\mathrm{C},1}$ to $E_{\mathrm{C},2}$ it will remain constant until $E_{\mathrm{C},2}$ or $E_{\mathrm{C},1}$ (depending upon the polarization direction) is reached, as shown in Fig. 1. Between the potentials $E_{\mathrm{C},1}$ and $E_{\mathrm{C},2}$, the ratio of the oxidized to the reduced form does not change at all. For several limiting concentrations of solid solutions, the separations between critical potentials are listed in Table 1. The separation will vanish if $Z_{\mathrm{red/ox}} = Z_{\mathrm{ox/red}} = 0.5$, i.e. if the components can be mixed in all ratios. The described behavior deserves further comments. From a strict thermodynamic point of view, one expects that the solid compound will segregate into two phases, one with the composition $Z_{\mathrm{red/ox}}$ and the other with the composition $Z_{\mathrm{ox/red}}$, when the electrode potential is within the range $E_{\mathrm{C},1}$ to $E_{\mathrm{C},2}$. This would happen if the two redox forms possessed sufficient solubility in the electrolyte solution. It would also happen if a thermodynamically unstable oversaturated solid mixed phase of a composition between $Z_{\mathrm{red/ox}}$ and $Z_{\mathrm{ox/red}}$ were formed, followed by a segregation into the stable phases. In many cases, both routes are closed, which could lead to an equilibration of the two phases of border composition. Thus the situation arises that because of an insolubility of red and ox in the electrolyte solution and because of the existence of a miscibility gap in the solid state (both are thermodynamic phenomena), there is no kinetically possible way to equilibrate the two phases. Simply said, the absence of dissolved species is the reason for the separation of the anodic and cathodic processes rather than nucleation kinetics as assumed by other authors [2–4].

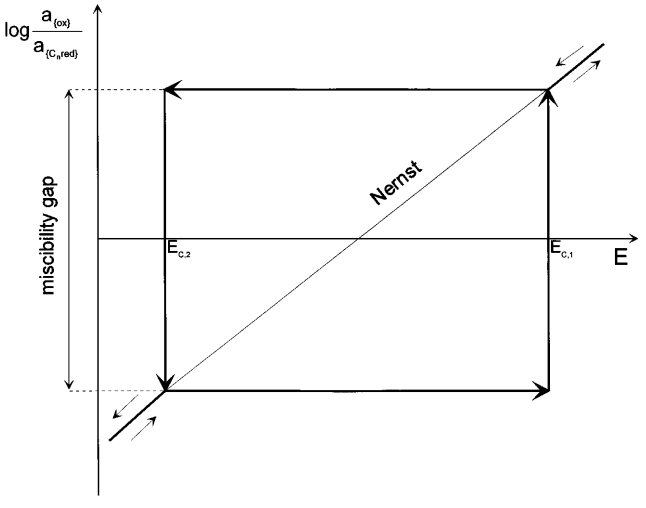

Fig. 1 Schematic plot of the logarithm of the activity ratios of the oxidized to the reduced form in the solid state as a function of electrode potential

The voltammetric response of systems with miscibility gaps

Simple case

The influence of this phenomenon in cyclic voltammetry is here investigated under the most simple conditions by using a planar, semiinfinite diffusion model. These conditions exist in a tall cylinder of the redox-active solid substance, which is pressed into an electrode surface in such a way that only one of its surfaces is exposed to the solution. The substance is a good electron conductor, and its surface in contact with the solution acquires the electrode potential at the very beginning of the experiment. Ions can diffuse through this surface along the longitudinal axis of the cylinder (see Fig. 2). If this axis is much longer than the diffusion layer, the semiinfinite diffusion model will apply. So the mass transfer can be described by the differential equation [7]

Table 1 Critical potentials $E_{\mathrm{C},1}$ and $E_{\mathrm{C},2}$ as a function of miscibility limits $Z_{\mathrm{red/ox}}$ and $Z_{\mathrm{ox/red}}$

$Z_{\mathrm{red/ox}}$	$n(E_{\mathrm{C},1}-E_{\mathrm{f}})$ (V)	$Z_{\mathrm{ox/red}}$	$n(E_{\mathrm{C},2}-E_{\mathrm{f}})$ (V)	$n(E_{\mathrm{C},1}-E_{\mathrm{C},2})$ (mV)
0.3	0.022	0.3	−0.022	44
0.2	0.036	0.2	−0.036	72
0.1	0.056	0.1	−0.056	112
0.05	0.076	0.05	−0.076	152
0.01	0.118	0.01	−0.118	236
0.005	0.136	0.005	−0.136	272

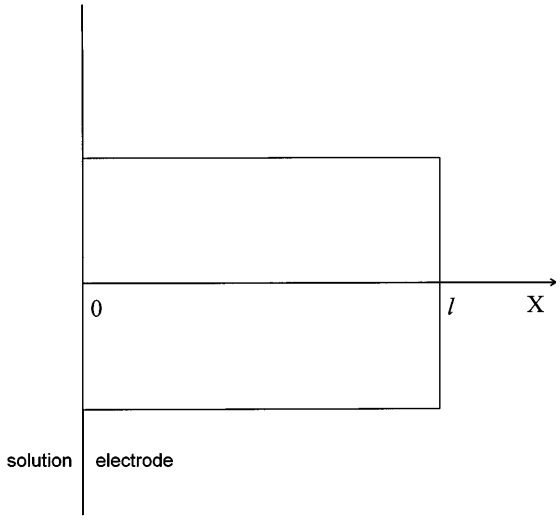

Fig. 2 A scheme of the solid electroactive microcylinder pressed into the working electrode surface

$$\partial c_{\mathrm{red}}/\partial t = D(\partial^2 c_{\mathrm{red}}/\partial x^2) \tag{17}$$

where the following conditions hold:

$$t = 0, \quad x \geq 0 : c_{\mathrm{red}} = 0,\ c_{\mathrm{ox}} = \rho \tag{a}$$
$$t > 0,\ x \to \infty : c_{\mathrm{red}} \to 0,\ c_{\mathrm{ox}} \to \rho \tag{b}$$
$$x \geq 0 : c_{\mathrm{ox}} + c_{\mathrm{red}} = \rho \tag{c}$$
$$x = 0 : c_{\mathrm{ox}} = c_{\mathrm{red}} \exp(\varphi) \tag{d}$$
$$(\partial c_{\mathrm{red}}/\partial x)_{x=0} = -i/nFSD \tag{e}$$
$$\varphi = \varphi_{\mathrm{St}} + at \tag{f}$$

where $\varphi_{\mathrm{St}} = (nF/RT)(E_{\mathrm{St}} - E_{\mathrm{f}})$, $a = (nF/RT)(\mathrm{d}E/\mathrm{d}t)$ and E_{St} are a starting potential in cyclic voltammetry; S is an area of the solid particle surface which is exposed to the solution and D a diffusion coefficient of ions C^+ in the crystal lattice. The solution of Eq. (17) is:

$$\int_0^t \left(i/nFSD^{1/2}\right)[\pi(t-\tau)]^{-1/2}\mathrm{d}\tau = [1+\exp(\varphi)]^{-1}\cdot\rho \tag{18}$$

It is numerically solved for staircase cyclic voltammetry (SCV) and linear-scan cyclic voltammetry (LSCV). In SCV, the potential is changed in the finite increments ΔE. The formal scan rate is defined as $v = \Delta E/\Delta t$, where Δt is the duration of each step. The current is sampled once at the end of each step. The numerical integration of Eq. (18) was performed by using the time increment $d = \Delta t/25$. A dimensionless current $\Phi = i(\Delta E)^{1/2}(nFS\rho)^{-1}(Dv)^{-1/2}$ is calculated by the following system of recursive formulae [8]

$$\Phi_1 = \left(5\pi^{1/2}/2\right)[1+\exp(\varphi_1)]^{-1} \tag{19}$$

$$\Phi_m = \left(5\pi^{1/2}/2\right)[1+\exp(\varphi_m)]^{-1} - \sum_{i=1}^{m-1}\Phi_i S_{m-i+1} \tag{20}$$

where $S_k = k^{1/2} - (k-1)^{1/2}$

In LSCV, the dimensionless current is defined as $\Phi = i(\mathrm{d}E)^{1/2}(nFS\rho)^{-1}(Dv)^{-1/2}$, where $\mathrm{d}E = 0.2\,\mathrm{mV}$ is a fixed potential increment.

Influence of finite volume of the substance

The influence of the finite volume of the redox-active substance is then investigated by the calculation of the mass transfer in a small hemispherical solid particle. The differential equation [9]

$$\partial(rc_{\mathrm{red}})/\partial t = D\left(\partial^2 rc_{\mathrm{red}}/\partial r^2\right) \tag{21}$$

is solved under the following initial and boundary conditions

$$t = 0,\ 0 \leq r \leq r_0 : c_{\mathrm{red}} = 0,\ c_{\mathrm{ox}} = \rho \tag{g}$$
$$t > 0, \qquad r = r_0 : (C_{\mathrm{red}})_{r=r_0} = \rho[1+\exp(\varphi)]^{-1} \tag{h}$$
$$(\partial c_{\mathrm{red}}/\partial r)_{r=r_0} = i/nFSD \tag{i}$$

where r_0 is the radius of the particle and $S = 2r_0^2\pi$ the area of its surface which is in the contact with the solution. For cyclic voltammetry, the solution of Eq. (21) is

$$\begin{aligned}
&[1+\exp(\varphi)]^{-1} + 2\sum_{p=1}^{\infty}\int_0^t [1+\exp(\varphi)]^{-1} pa(t-\tau)^{-1} \\
&\quad\times (2\pi^{1/2})^{-1}(t-\tau)^{-1/2}\cdot\exp\left[-p^2a^2(t-\tau)^{-1}/4\right]\mathrm{d}\tau \\
&\quad - D^{1/2}r_0^{-1}\int_0^t [1+\exp(\varphi)]^{-1}\pi^{-1/2}(t-\tau)^{-1/2}\mathrm{d}\tau \\
&\quad = \int_0^t \left(i/nFS\rho D^{1/2}\right)\pi^{-1/2}(t-\tau)^{-1/2}\mathrm{d}\tau
\end{aligned} \tag{22}$$

where $a = 2r_0D^{-1/2}$. For numerical integration, Eq. (22) can be transformed into a system of recursive formulae

$$\begin{aligned}
\Phi_l = &\left(5\pi^{1/2}/2\right)[1+\exp(\varphi_1)]^{-1} \\
&+ 5\pi^{1/2}Q_l[1+\exp(\varphi_1)]^{-1} - 5(r^*)^{-1}[1+\exp(\varphi_1)]^{-1}
\end{aligned} \tag{23}$$

$$\begin{aligned}
\Phi_m = &\left(5\pi^{1/2}/2\right)[1+\exp(\varphi_m)]^{-1} \\
&+ 5\pi^{1/2}\sum_{i=1}^{m}[1+\exp(\varphi_i)]^{-1}Q_{m-i+1} \\
&- 5(r^*)^{-1}\sum_{i=1}^{m}[1+\exp(\varphi_i)]^{-1}S_{m-i+1} - \sum_{i=1}^{m-1}\Phi_i S_{m-i+1}
\end{aligned} \tag{24}$$

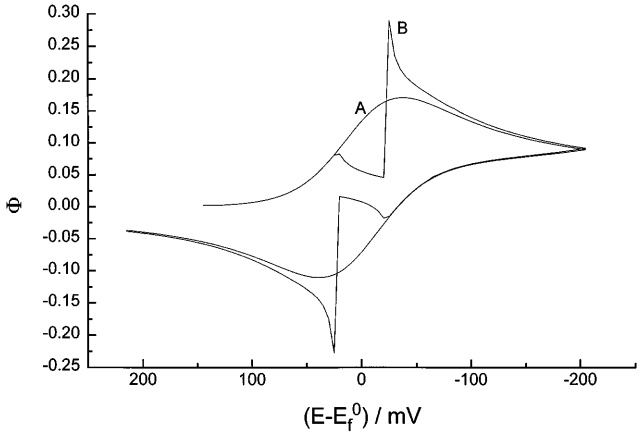

Fig. 3 Staircase cyclic voltammograms of ideally miscible **(A)** and partly immiscible **(B)** solid redox components. Miscibility limits: $Z_{red/ox} = Z_{ox/red} = 0.5$ (*1*) and 0.3 (*2*). Reversible redox reaction, $\Delta E = 5\,mV$, planar, semiinfinite diffusion model

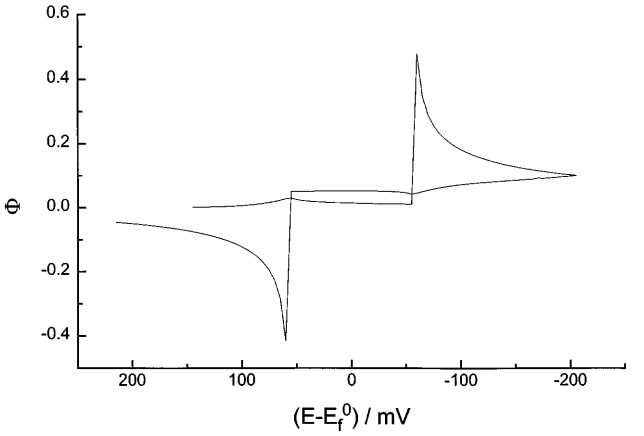

Fig. 4 Staircase cyclic voltammetry (SCV) of a reversible solid-state redox reaction influenced by the limited miscibility of the components. $Z_{red/ox} = Z_{ox/red} = 0.1$. All other data as in Fig. 3

where $Q_1 = R_1$, $Q_k = R_k - R_{k-1}$, $R_k = \sum_{p=1}^{\infty} erfc\,[pr^* k^{-1/2}]$ \quad and $r^* = 5r_0 v^{1/2}(D\Delta E)^{-1/2}$ is a dimensionless radius of the particle.

Influence of redox kinetics

The influence of redox kinetics is investigated by using the semiinfinite, planar diffusion model. Based on the condition

$$i/nFS = k_S \exp(-\alpha\varphi)\left[(c_{ox})_{x=0} - (c_{red})_{x=0}\exp(\varphi)\right] \qquad \text{(j)}$$

instead of Condition d, the solution of Eq. 8 is obtained in the form of recursive formulae [10]

$$\Phi_l = \kappa\exp(-\alpha\varphi_l)[1 + \kappa\omega\exp(-\alpha\varphi_l)(1 + \exp(\varphi_l))]^{-1} \qquad (25)$$

$$\Phi_m = \left[\kappa\exp(-\alpha\varphi_m) - \kappa\exp(-\alpha\varphi_m)(1 + \exp(\varphi_m))\omega \sum_{i=1}^{m-1}\Phi_i S_{m-i+1}\right]\cdot[1 + \kappa\omega\exp(-\alpha\varphi_m)(1 + \exp(\varphi_m))]^{-1} \qquad (26)$$

where $\kappa = k_s(\Delta t/D)^{1/2}$ is a dimensionless kinetic parameter and $\omega = 2/5\pi^{1/2}$.

Results and discussion

The influence of the limited miscibility of redox components of the mixed crystal on staircase cyclic voltammograms simulated with the aid of the semiinfinite diffusion model is shown in Fig. 3. Curve A is the voltammogram of the components which can be mixed in all ratios, and curve B corresponds to the equal maximum miscibility $Z_{red/ox} = Z_{ox/red} = 0.3$. The maximum miscibility $Z_{red/ox} = 0.3$ means that the mixed crystal is saturated with $\{C_n red\}$ when 30% of $\{ox\}$ is reduced. As can be seen in Fig. 3, the saturation causes a splitting of both the cathodic and the anodic branches of the voltammogram into two peaks. The first peak appears when the surface of the crystal is charged to the first critical potential $E_{C,1}$. Although the potential of the electrode is continuously changed, the ratio of the oxidized to the reduced form remains constant and equal to its value at $E_{C,1}$ until the electrode potential is equal to the second critical potential $E_{C,2}$ (see Fig. 1). So in this potential range the response of the crystal corresponds to the electrolysis at a constant potential, i.e. it decreases in proportion to the square root of the time which is needed to expand the diffusion layer through the crystal. This is the origin of the first peak. When the electrode potential is equal to $E_{C,2}$, at this moment the composition of the crystal surface suddenly changes from 30% $\{C_n red\}$ and 70% $\{ox\}$ to 70% $\{C_n red\}$ and 30% $\{ox\}$. This sudden reduction of 40% of the surface concentration of $\{ox\}$ is manifested as a sharp peak on the cathodic branch of the voltammogram. As the electrode potential is changed in discrete increments, the potential of this sharp peak in SCV is not exactly equal to $E_{C,2}$, but to the potential of the first step, which is more negative than $E_{C,2}$. In Fig. 3, it is $E_P = -0.025\,V$ vs E_f, while $E_{C,2} = -0.02175\,V$ vs E_f because $\Delta E = 5\,mV$. After reaching the sharp maximum, the current decreases as the diffusion layer extends into the crystal body. In the anodic branch, the response is symmetrical. The first smaller peak appears at $E_{C,2}$ and the bigger sharp one at $E_{C,1}$.

The separation between the sharp cathodic and anodic peaks increases as the miscibility of the components decreases. This is shown in Figs. 4 and 5, for $Z_{red/ox} = Z_{ox/red} = 0.1$ and 0.01, respectively. Also, the

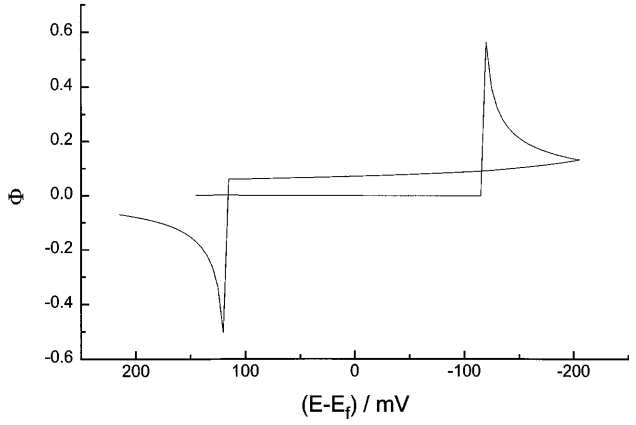

Fig. 5 As Fig. 4, but $Z_{red/ox} = Z_{ox/red} = 0.01$

ratio between the first smaller peak and the second higher peak in each of the branches of voltammograms decreases as the miscibility becomes smaller. If the maximum miscibility is lower than 10% , the first peak can be neglected and the voltammogram will consist only of two well-separated sharp reduction and oxidation peaks. The inversion of the current in the anodic branch of the voltammogram (a cathodic current in the anodic scan before the oxidation peak) is the consequence of the experimental conditions. It depends on the final potential, at which the scan is reversed, and on the assumed semiinfinite diffusion model.

The dependence of the cathodic peak current on the peak potential is shown in Fig. 6. It has the form of a logarithmic function. If the immiscibility overvoltage is higher than 100 mV, the peak current will depend on diffusion parameters and not on the miscibility.

If there is no immiscibility polarization, the cathodic and the anodic peak potentials will be separated by $70/n$ mV for 5-mV potential steps (cf. [11]). A small polarization ($z_{B/A} = z_{A/B} = 0.3$) even decreases this separation but increases the peak currents.

In reality, solid redox substances will rarely have equal critical potentials ($E_{C,1}$ and $E_{C,2}$). It is more probable that they will be different, as a consequence of different miscibilities of the redox components. Two examples are shown in Figs. 7 and 8. The mid-potentials of these responses $E_m = (E_{P,a} + E_{P,c})/2$ are not equal to the formal potential E_f of the redox reaction (Eq. 1), which is of great importance for the derivation of formal potentials from cyclic voltammograms. Figure 9 shows that in LSCV, peak potentials are exactly equal to critical potentials and peak currents are almost ten times those in staircase cyclic voltammetry. These currents are very sharp "needles" which are not wider than 0.4–0.6 mV. The rest of the response is the diffusion controlled "tail" which is similar to the response in staircase voltammetry.

The influence of the finite crystal volume on the staircase cyclic voltammogram is shown in Fig. 10. Miscibility parameters are the same as those in Fig. 4 ($Z_{red/ox} = Z_{ox/red} = 0.1$), but the results in Fig. 10 are calculated for a very small hemispherical particle with the dimensionless radius $5r_0v^{1/2}(D\Delta E)^{-1/2} = 20$. The main difference between Fig. 4 and Fig. 10 is that such small particles can be electrolyzed exhaustively within a single potential scan. The peaks are thus more narrow, without distinct diffusion "tails", and the current between the cathodic and the anodic peaks tends to be zero.

The dependence of the peak currents of small hemispherical particles on their dimensionless radii in SCV is shown in Fig. 11. There are very small responses of very small crystals as a consequence of the current sampling procedure which is used in this technique. The redox components of the particles react at the very beginning of the potential step, and the current which is measured at the end of the step is small. As the radius increases, the diffusion of ions prolongs the redox reaction within the crystal and the peak current increases. The influence of the finite volume of the particle will be negligible if $5r_0v^{1/2}(D\Delta E)^{-1/2} > 10^3$.

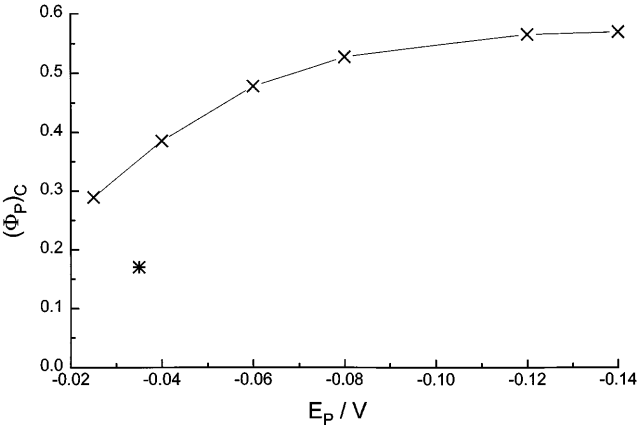

Fig. 6 Dependence of dimensionless cathodic peak current influenced by the miscibility polarization on the peak potentials (or the peak separation). $\Delta E = 5$ mV, planar, semiinfinite diffusion model, $E_{C,1} = E_{C,2}$. The *asterisk* applies to $E_{C,1} = E_{C,2} = OV$

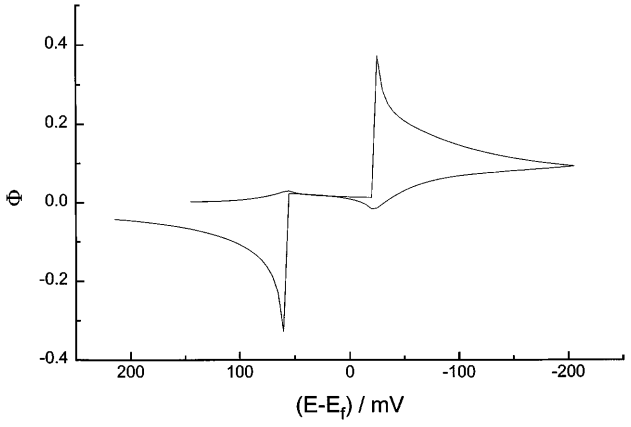

Fig. 7 All as Fig. 4, but $Z_{red/ox} = 0.1$ and $Z_{ox/red} = 0.3$

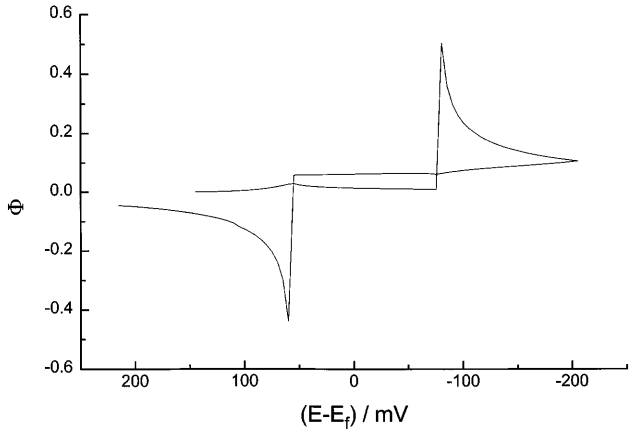

Fig. 8 All as Fig. 4, but $Z_{red/ox} = 0.1$ and $Z_{ox/red} = 0.05$

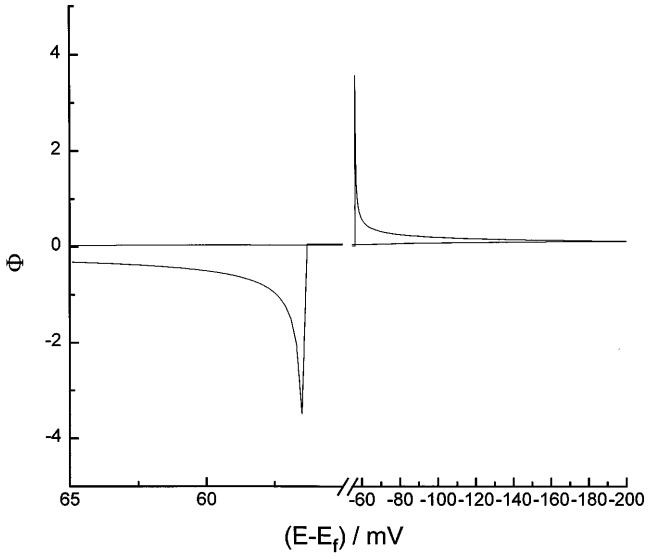

Fig. 9 Linear scan cyclic voltammogram of a reversible solid state redox reaction influenced by the miscibility polarization: $Z_{red/ox} = Z_{ox/red} = 0.1$

In LSCV, the current is measured continuously and the response of microparticles consists of two very high, sharp and narrow peaks which appear at the critical potentials. This is shown in Fig. 12 for the hemispherical particle with the dimensionless radius equal to 10. Curve A is the voltammogram in the absence of the immiscibility polarization, and curve B is the response which is influenced by the limited miscibility ($Z_{red/ox} = Z_{ox/red} = 0.1$). Two main peaks of this response are shown only partly because their peak currents are a hundred times as large as the maxima of curve A. However, the widths of these peaks are only 5 mV.

The sharp maxima which appear as a consequence of the immiscibility polarization are very sensitive to the redox kinetics, as can be seen in Fig. 13. This figure shows theoretical quasi-reversible voltammograms as calculated by the planar, semiinfinite diffusion model. The dimensionless kinetic parameter of the redox reaction $\kappa = 0.1$ is shown in Fig. 13A and that of $\kappa = 0.05$ in Fig. 13B. The curves marked "1" in Fig. 13A and B correspond to the ideally miscible components ($Z_{red/ox} = Z_{ox/red} = 0.5$), and the curves marked "2" are the voltammograms influenced by their limited miscibility ($Z_{red/ox} = Z_{ox/red} = 0.1$). Figure 13 is to be compared with Figs. 3 (curve 1) and 4. If there is no immiscibility polarization, the cathodic peak potentials of quasi-reversible staircase voltammograms are -0.1 V, if $\kappa = 0.1$ and -0.135 V, if $\kappa = 0.05$, which can be compared to $E_P = -0.035$ V for the reversible redox reaction. If $\kappa = 0.1$ and the solubility of the solid redox component is limited, the cathodic peak potential is -0.060 V, which is close to the critical potential $E_{C,2} = -0.0564$ V, but the peak current is smaller and the peak is wider than in the case of the reversible redox reaction (compare curve 2 in Fig. 13A with Fig. 4). If $\kappa = 0.05$, the current will increase sharply at the critical

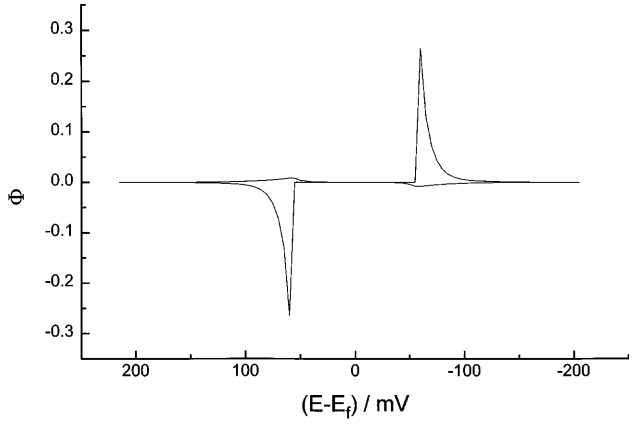

Fig. 10 SCV of a small hemispherical solid electroactive microparticle with a dimensionless radius $5r_0v^{1/2}(D\Delta E)^{-1/2} = 20$. Reversible redox reaction influenced by the limited miscibility of components: $Z_{red/ox} = Z_{ox/red} = 0.1$

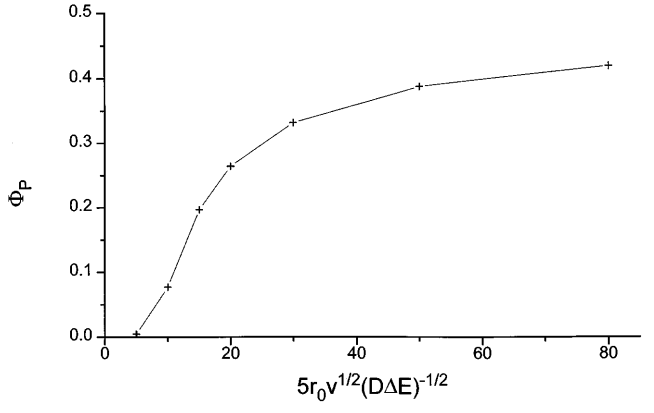

Fig. 11 Dependence of dimensionless cathodic peak currents in staircase voltammetry on dimensionless radii of small hemispherical electroactive solid particles. Reversible redox reaction, $\Delta E = 5$ mV and $Z_{red/ox} = Z_{ox/red} = 0.1$

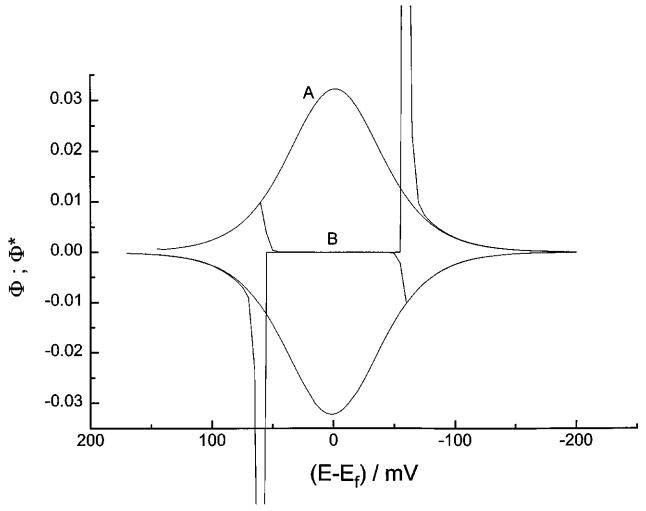

Fig. 12A, B Linear scan cyclic voltammetry (LSCV) of a small hemispherical solid particle with the dimensionless radius $r_0(v)^{1/2}(D \cdot \mathrm{d}E)^{-1/2} = 10$. Reversible redox reaction, $\mathrm{d}E = 0.2\,\mathrm{mV}$. **A** The redox components of the particle are mutually ideally miscible. **B** The system has a large miscibility gap ($Z_{\mathrm{red/ox}} = Z_{\mathrm{ox/red}} = 0.1$)

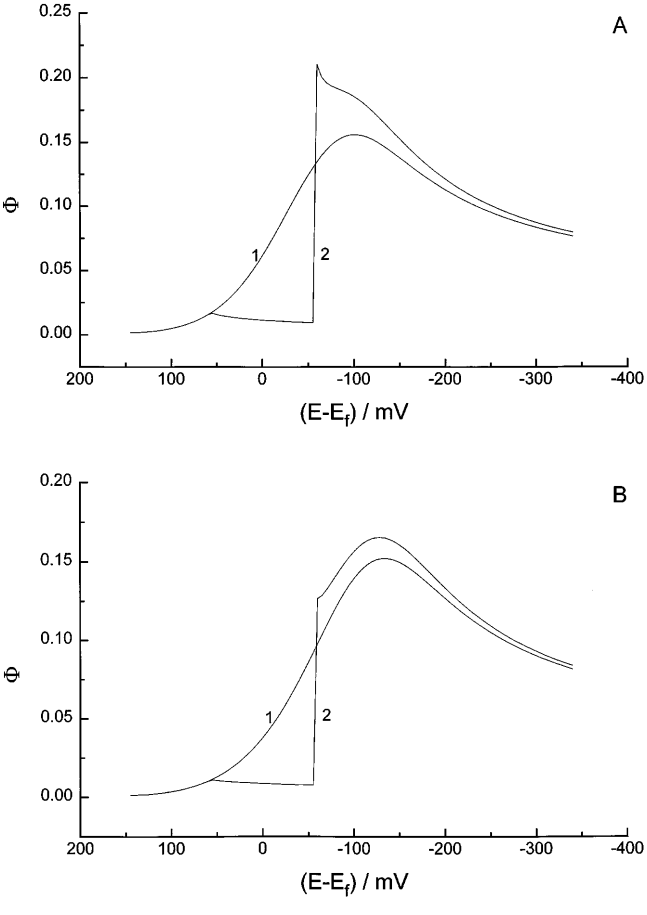

Fig. 13A, B Influence of redox kinetics on staircase voltammograms of ideally miscible (*1*) and partly immiscible ($Z_{\mathrm{red/ox}} = Z_{\mathrm{ox/red}} = 0.1$) (*2*) redox components of the solid mixed phase. Dimensionless redox reaction rate constant $k_S(\Delta t/D)^{1/2} = 0.1$ **(A)** and 0.05 **(B)**. Charge-transfer coefficient $\alpha = 0.5$ and potential increment $\Delta E = 5\,\mathrm{mV}$. Planar, semiinfinite diffusion model

potential, but will then continue to increase slowly until the maximum appears at $-0.125\,\mathrm{V}$ (see Fig. 13B). This is caused by the relatively slow response of the kinetically controlled redox reaction to the sudden change of the potential from $E_{C,1}$ to $E_{C,2}$. If the reaction is irreversible ($\kappa < 0.01$), the voltammograms will exhibit no increase in current at the critical potential.

Conclusions

The transformation of an oxidized solid compound into a reduced solid compound and vice versa can be described on the basis of the formation of mixed crystals between both redox forms. Especially in the case of intercalation electrochemistry, there are examples of systems which form a continuous series of mixed crystals between the oxidized and reduced forms. X-ray data support this for Prussian blue and related compounds, which show only marginal changes of lattice constants of the fully reduced and oxidized compounds. Similarity of the lattice structure is the major prerequisite for the formation of mixed crystals. There are other solid state systems which exhibit marked differences between the crystal structure of different redox forms. In view of the present results, the electrochemistry of solid 7, 7, 8, 8 – Tetracyanoquinodimethane (TCNQ) [3, 4] can be interpreted in terms of the miscibility of the TCNQ with its reduced and ion-intercalated forms. Bond and coworkers [1, 4] provide the structures of {TCNQ}, $\{Na^+TCNQ^-\}$, $\{K^+TCNQ^-\}$, $\{Rb^+TCNQ^-\}$ and $\{(Cs^+)_2(TCNQ^-)_2$ TCNQ$\}$. The crystal structures of {TCNQ} and $\{(Cs^+)_2$ $(TCNQ^-)_2$ TCNQ$\}$ show the largest deviations from each other. They also give the largest separation between the anodic and cathodic peaks (250 mV). {TCNQ} and $\{K^+TCNQ^-\}$ are most similar with respect to their structure and they exhibit the smallest peak separation (125 mV). As the similarity of structure determines to a great extent their miscibility, it is easy to understand the solid state electrochemical behavior of these systems. Figure 14 depicts how a real voltammogram may deviate from the theoretically calculated voltammograms due to well-known kinetic processes. This figure shows the oxidation of a phase $\{C_n\mathrm{red}\}$ with a structure denoted by α. This compound is partially oxidized at $E_{C,2}$ giving rise to signal 1. In reality, it might be possible that the oxidation proceeds further and an oversaturation is achieved which will give signal 1a. Signal 1a will be better developed at fast polarization rates as this will lead to higher degrees of oversaturation. When phase α is saturated with {ox}, it needs to undergo a phase transition to phase β, which consists of an excess of {ox} with some $\{C_n\mathrm{red}\}$ as a dissolved component. From a thermodynamic point of view, this phase transition can occur only at $E_{C,1}$ when the solution pathway is closed due to insolubility. Certainly, in reality, phase transitions can be accompanied by complicated nucle-

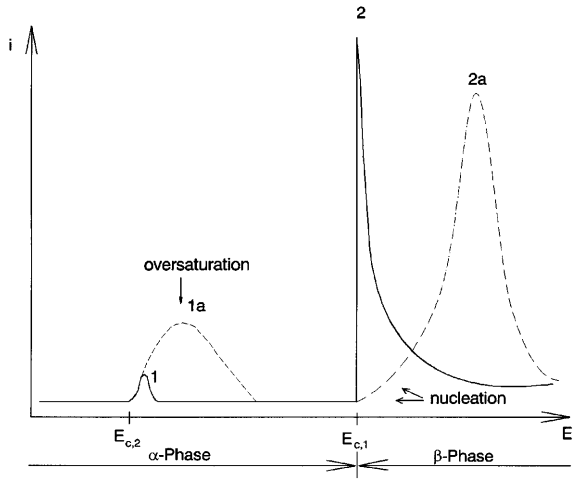

Fig. 14 Schematic voltammogram for the case of a solid system with a miscibility gap including the kinetic phenomena of oversaturation and nucleation overvoltage

ation processes, and also by a nucleation overvoltage. This phenomenon will modify the sharp peak 2 to a broadened peak 2a as shown in Fig. 14. Thus, nucleation overvoltage is certainly involved in many solid-state electrochemical transitions, but it is more likely that the large separations between $E_{P,ox}$ and $E_{P,red}$ are usually due to the miscibility gaps and insolubility. The nucleation overvoltage amounts to some mV only in case of the nucleation of solids from solutions [12], but this amount may be much larger for the nucleation of a solid phase into another solid phase. This area deserves very careful experimental studies for which the present work is hoped to be helpful. In the context of the present discussion, it is no longer surprising that the reduction of silver halides to silver could be successfully simulated by a model involving mixed phase thermodynamics with respect to AgX-Ag [5]. It may be suspected that most metal oxide/metal, metal sulfide/metal and metal salt/metal systems can be described with this model of mixed-phase formation in the sense of $\{Ox_xRed_{1-x}\}$, including large miscibility gaps.

Generally, it can be said that redox mixed phases have not yet been studied sufficiently, not to mention solid-solid phase transitions and phase nucleation in the course of solid-state electrochemical reactions. Our knowledge of these phenomena is far behind that of alloys [13], which have been investigated for several decades.

Acknowledgements We acknowledge support by the respective Ministries in the framework of a bilateral German-Croatian Scientific Research Program and by Fonds der Chemischen Industrie.

References

1. Babano JP (ed) (1983) Lithium batteries. Academic, London
2. Shaw SJ, Marken F, Bond AM (1996) Electroanalysis 8: 732
3. Chambers JQ, Scaboo K, Evans CD (1996) J Electrochem Soc 143: 3039
4. Bond AM, Fletcher S, Marken F, Shaw SJ, Symons PG (1996) J Chem Soc Faraday Trans 92: 3925
5. Jaworski A, Stojek Z, Scholz F (1993) J Electroanal Chem 354: 1
6. Weppner W (1995) In: Bruce PG (ed) Solid state electrochemistry. Cambridge University Press, Cambridge, pp 199–228
7. Galus Z (1976) Fundamentals of electrochemical analysis. Wiley, New York, p. 63
8. Nicholson RS, Olmstead ML (1972) In: Mattson JS, Mark HB, McDonald HC (eds) Electrochemistry: calculations, simulation and instrumentation, vol 2. Dekker, New York, p. 119
9. Vasilieva LN, Vinogradova EN (1961) Zavod Lab 27: 1079
10. Lovrić M, Komorsky-Lovrić Š , Scholz F (1997) Electroanalysis 9: (in press)
11. Christie JH, Lingane PJ (1965) J Electroanal Chem 10: 176
12. Budevski E, Staikov G, Lorenz WJ (1996) Electrochemical phase formation and growth, an introduction to the initial stages of metal deposition. VCH, New York
13. Much GE (ed) (1985) Phase Stability and Phase Transformation. (Materials science forum, vol 3) Trans Tech Publications, Switzerland